PLK1 depletion alters homologous recombination and synaptonemal complex disassembly events during mammalian spermatogenesis

Stephen R. Wellard, Marnie W. Skinner‡, Xueqi Zhao‡, Chris Shults‡, and Philip W. Jordan*
Biochemistry and Molecular Biology Department, Johns Hopkins University Bloomberg School of Public Health, Baltimore, MD 21205

ABSTRACT Homologous recombination (HR) is an essential meiotic process that contributes to the genetic variation of offspring and ensures accurate chromosome segregation. Recombination is facilitated by the formation and repair of programmed DNA double-strand breaks. These DNA breaks are repaired via recombination between maternal and paternal homologous chromosomes and a subset result in the formation of crossovers. HR and crossover formation is facilitated by synapsis of homologous chromosomes by a proteinaceous scaffold structure known as the synaptonemal complex (SC). Recent studies in yeast and worms have indicated that polo-like kinases (PLKs) regulate several events during meiosis, including DNA recombination and SC dynamics. Mammals express four active PLKs (PLK1–4), and our previous work assessing localization and kinase function in mouse spermatocytes suggested that PLK1 coordinates nuclear events during meiotic prophase. Therefore, we conditionally mutated *Plk1* in early prophase spermatocytes and assessed stages of HR, crossover formation, and SC processes. *Plk1* mutation resulted in increased RPA foci and reduced RAD51/DMC1 foci during zygonema, and an increase of both class I and class II crossover events. Furthermore, the disassembly of SC lateral elements was aberrant. Our results highlight the importance of PLK1 in regulating HR and SC disassembly during spermatogenesis.

INTRODUCTION

Meiosis is an essential cell cycle required by all reproducing mammals for gametogenesis, which involves one round of DNA replication and two rounds of cell division to ultimately generate four haploid gametes. After completing chromosome replication in the premeiotic S phase, a primary germ cell undergoes homologous chromosome synapsis during prophase I. Synapsis between homologous chromosomes is facilitated by a zipper-like protein structure called the synaptonemal complex (SC; Zickler and Kleckner, 1999). The SC is made up of lateral and central elements. Lateral elements consist of SYCP2, SYCP3, and cohesins, which form axes between sister chromatids. Homologous chromosome pairs are synapsed by bridging the lateral elements via central region proteins. The central region of the SC contains traverse filament, SYCP1, and central elements, SYCE1/2/3, SIX6OS1, and TEX12 (Costa and Cooke, 2007; Fraune *et al.*, 2012; Bolcun-Filas and Handel, 2018). SC assembly and disassembly processes are divided into five substages of prophase I, known as leptonema, zygonema, pachynema, diplonema, and diakinesis. At leptonema, SYCP2 and SYCP3 form axial elements between each pair of sister chromatids, with cohesins underlying the framework for axial element formation (Fraune *et al.*, 2012). By zygonema, central elements start to form between homologous chromosomes. At the pachytene stage, the SC is fully assembled along the axis of homologous chromosomes. By diplonema,

SC central region proteins dissociate but remain at the centromere and sites of crossover recombination. By diakinesis, central region proteins are absent and lateral elements disassemble from arms but persist at the kinetochore (Cahoon and Hawley, 2016).

Concomitant with synapsis, homologous chromosomes undergo DNA recombination. During leptonema, the homologous recombination (HR) process is initiated by the formation of double-strand breaks (DSBs), induced by an evolutionarily conserved DNA topoisomerase, SPO11-TOPOVIBL (Bergerat et al., 1997; Keeney et al., 1997; Cole et al., 2010; Robert et al., 2016). DSB formation is aided by localization of HORMAD1 on unsynapsed axes. HORMAD1 together with meiosis-specific interacting proteins, CCDC36 (IHO1), MEI4, and REC114 form a complex to promote DSB formation (Stanzione et al., 2016). DSB formation stimulates the DNA damage response (DDR) signaling cascade directed by ataxia telangiectasia mutated (ATM) and Rad3-related (ATR) kinases. ATM and ATR phosphorylate histone H2AFX (γH2AX) and recruit other DDR proteins including the ATR interacting protein (ATRIP; Bellani et al., 2005; Refolio et al., 2011; Royo et al., 2013). DSBs undergo single-strand resection to form 3′ single-stranded DNA (ssDNA) overhangs that are bound by ssDNA binding complexes RPA and MEIOB-SPATA22 (Luo et al., 2013; Shi et al., 2019). RPA localization is instrumental for recruitment of DNA recombinases RAD51 and DMC1, which enable 3′ ssDNA overhangs to undergo strand exchange between homologues, referred to as single-end invasions, forming D-loop recombination intermediates (Hunter and Kleckner, 2001; Sansam and Pezza, 2015). D-loop intermediates are processed via noncrossover and crossover pathways, also known as the synthesis-dependent strand annealing (SDSA) model and the double-strand break repair (DSBR) model, respectively (Szostak et al., 1983; McMahill et al., 2007). During SDSA, the invading 3′ ssDNA of the D-loop is extended via DNA replication, then subsequently displaced via BLM helicase to anneal to the other ssDNA end of the DSB, followed by gap-filling DNA synthesis and ligation. In contrast, DSBR involves the formation of double-Holliday junctions (dHJs) that form when the other end of the DSB is also captured within the recombination intermediate. After gap repair, dHJs can be resolved to form crossovers or noncrossovers.

In mammals, ~10–25% of meiotic DSBs are strictly controlled to produce crossovers (Reynolds et al., 2013). At least one crossover event occurs per homologous chromosome pair, which is defined as crossover assurance or obligatory crossover (Shinohara et al., 2008). In addition, multiple crossovers do not form near one another, which is a process referred to as crossover interference (Hunter, 2015). Most crossovers are generated by the interference-dependent (class I) pathway (Holloway et al., 2008). Class I crossover formation is achieved by recruitment of a complex of recombination factors, including MutS (MSH4-MSH5), RNF212, MutL (MLH1/3), CDK2, and HEI10. MSH4-MSH5 bind discretely at various recombination sites along homologous chromosomes at the pachytene stage (Kneitz et al., 2000). Meanwhile, RNF212, a central meiotic procrossover factor, selectively localizes onto MSH4-MSH5 sites to stabilize D-loops and form dHJs. RNF212-dependent SUMO modification further prevents the MSH4-MSH5-RNF212 complex from dissociation (Reynolds et al., 2013). Approximately half of MSH4-MSH5 marked sites progress into crossover sites, with the other half, without the stabilization of RNF212, being processed to form noncrossovers (Santucci-Darmanin et al., 2000; Reynolds et al., 2013). Cyclin-dependent kinase, CDK2, and an E3 ubiquitin ligase, HEI10, associate with MSH4-MSH5 –RNF212 marked foci to assist binding of MLH1/3, which is proposed to mark class I crossover sites (Anderson et al., 1999; Lipkin et al., 2002; Ward et al., 2007). A small subset of crossovers, ~5–10%, are formed by the alternative class II pathway, where MUS81-EME1 heterodimers function as an HJ resolvase responsible for resolving X-shaped joint molecules (Boddy et al., 2001; Holloway et al., 2008, 2011).

In addition to CDK2, polo-like kinases (PLKs) have been linked with a role of mediating crossover recombination events. In budding yeast, Cdc5 is required for SC disassembly and the resolution of dHJs during meiosis contributing to the activation of class I and class II crossover pathways via its kinase activity (Clyne et al., 2003; Sourirajan and Lichten, 2008; Matos et al., 2011; Argunhan et al., 2017; Wild et al., 2019). Caenorhabditis elegans express three PLKs of the same subfamily, PLK-1, 2, and 3 (de Cárcer et al., 2011). PLK-1 and PLK-2 have been shown to be important for regulating DSB formation and crossover designation (Machovina et al., 2016; Nadarajan et al., 2017; Brandt et al., 2020). In addition, PLK-1 and PLK-2 are required for mediating chromosome pairing and synapsis (Harper et al., 2011; Labella et al., 2011; Nadarajan et al., 2017). Mammals express four kinase proficient PLKs (PLK1–4). Using small molecule kinase inhibitors, it has been demonstrated that inhibition of PLK1 prevents normal SC disassembly (Ishiguro et al., 2011; Jordan et al., 2012). However, a role for PLK1 in meiotic recombination had not previously been assessed. Using a Plk1 conditional knockout (cKO) approach we assessed the role of PLK1 during meiotic recombination, and homologous chromosome synapsis and desynapsis. We report that Plk1 cKO spermatocytes undergo abnormal disassembly of the lateral elements of the SC and cause perturbations during meiotic recombination that result in increased crossover recombination levels.

RESULTS

Conditional knockout of Plk1 in spermatocytes results in infertility

As PLK1 is essential for early embryonic development (Lu et al., 2008), we used a cKO strategy for mutating Plk1 (see Materials and Methods). Exon 3 of Plk1 was flanked by Cre recombinase target sequences, and this allele was termed Plk1 flox. By breeding mice expressing the Cre recombinase to mice heterozygous for the Plk1 flox allele, we generated a KO allele termed Plk1 del. The heterozygous Plk1 del mice exhibited no gross morphological abnormalities during development and adult life. No homozygous offspring for the Plk1 del allele were produced in our study (n = 83 pups [15 litters] from crosses between heterozygote Plk1 del mice; 55 pups were Plk1 del heterozygotes and 28 pups were homozygous for the wild-type Plk1 allele), indicating that homozygosity for the deletion allele is lethal.

To determine the requirement for Plk1 during meiotic prophase of spermatogenesis, we used the Spo11 promoter to specifically express the Cre recombinase transgene in germ cells. Spo11-Cre is expressed as early as 10 days postpartum (dpp), which corresponds to early prophase, preleptotene/leptotene stage spermatocytes (Lyndaker et al., 2013; Hwang et al., 2018; Wellard et al., 2020). From analysis of hematoxylin and eosin (H&E) stained testis sections of adult control and Plk1 cKO male mice, it was evident that primary spermatocytes were undergoing cell cycle arrest during meiosis I, as round and elongating spermatids were never observed in Plk1 cKO tubules (Figure 1A). STA-PUT density sedimentation was used to purify mid to late prophase spermatocytes from control and Plk1 cKO testes. PLK1 protein levels and activation were then assessed via Western blot (Figure 1B). PLK1 activation was detected by using an antibody that specifically recognizes phosphorylation of the serine 137 residue (Phospho-PLK1 [Ser137]). Total PLK1 levels and PLK1 activation were greatly reduced in Plk1 cKO spermatocytes compared with controls. In contrast, the levels of SC lateral element
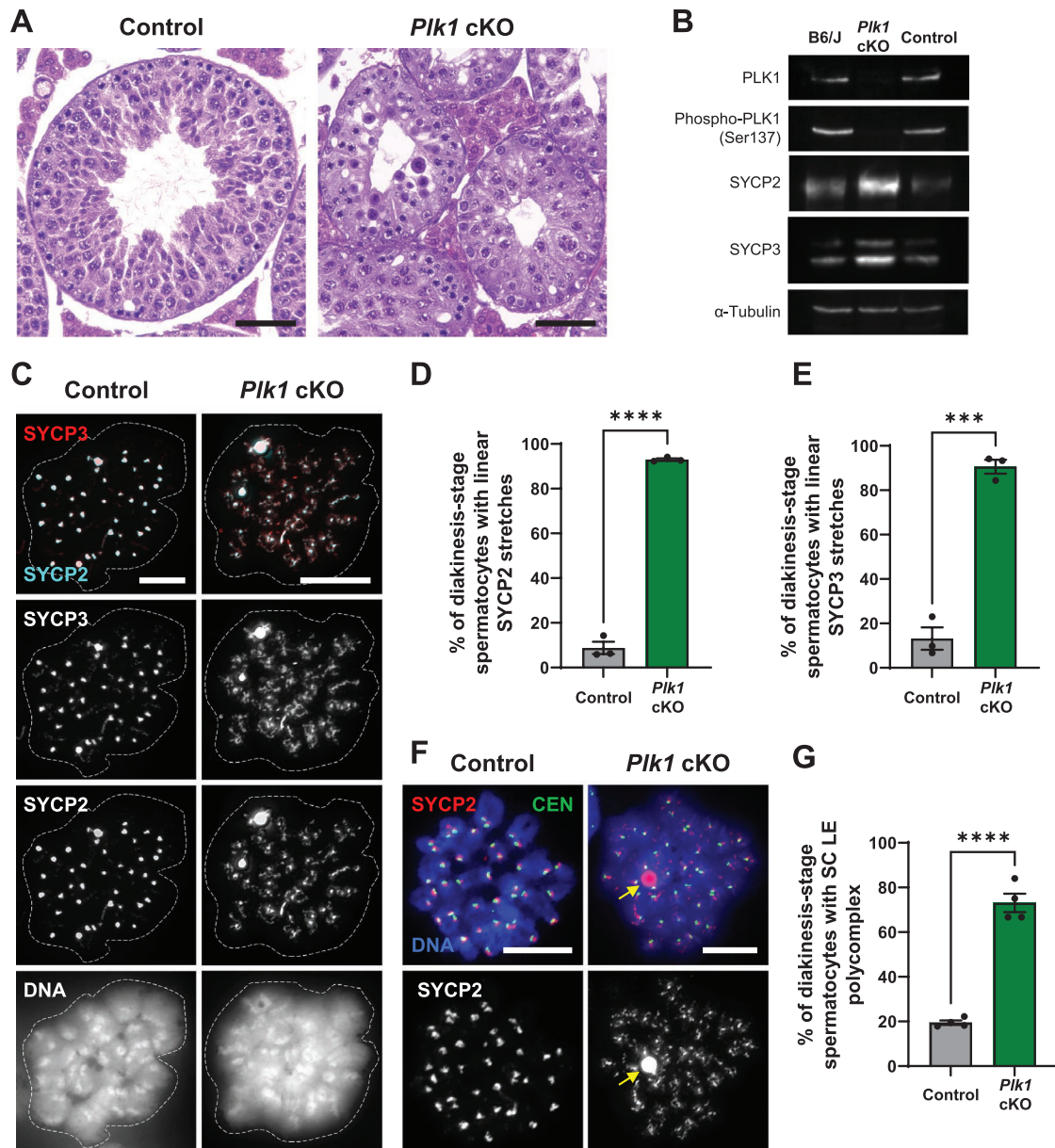
FIGURE 1: *Plk1* cKO spermatocytes display aberrant disassembly of SC lateral elements during the transition from diplonema to diakinesis. (A) H&E staining of 5-μm- thick testis sections of adult control and *Plk1* cKO mice. Scale bars = 50 μm. (B) Protein extracts from STA-PUT-isolated midlate prophase spermatocytes were collected from control and *Plk1* cKO mice. Isolation via STA-PUT density sedimentation resulted in 90% pure midprophase spermatocyte enrichment. Western blot analysis was performed for PLK1, Phospho-PLK1 (Ser137), SYCP2, SYCP3, and α-Tubulin as a loading control. (C) Representative chromatin spread preparations of diakinesis-stage spermatocytes from control and *Plk1* cKO mice immunolabeled with SYCP3 (red) and SYCP2 (cyan), and stained with DAPI (white, lower panel). Scale bars = 10 μm. (D) The percent of diakinesis-stage spermatocytes containing linear stretches of SYCP2 was quantified from three biological replicates in control (95 cells assessed) and *Plk1* cKO (70 cells assessed) mice. Error bars show mean ± SEM. *P* values (two-tailed Student's *t* test) comparing *Plk1* cKO to the control are indicated by ****, $P < 0.0001$. (E) The percent of diakinesis-stage spermatocytes containing linear stretches of SYCP3 was quantified from three biological replicates in control (110 cells assessed) and *Plk1* cKO (79 cells assessed) mice. Error bars show mean ± SEM. *P* values (two-tailed Student's *t* test) comparing *Plk1* cKO to the control are indicated by ***, $P < 0.001$. (F) Representative chromatin spread preparations of diakinesis-stage spermatocytes from control and *Plk1* cKO mice immunolabeled with SYCP2 (red), centromere (CEN; green), and stained with DAPI (blue). Yellow arrow pointing to a polycomplex of SYCP2. Scale bars = 10 μm. (G) The percent of diakinesis-stage spermatocytes containing lateral element polycomplexes in control (103 cells assessed) and *Plk1* cKO (76 cells assessed) mice. Error bars show mean ± SEM. *P* values (two-tailed Student's *t* test) comparing *Plk1* cKO to the control are indicated by ****, $P < 0.0001$.

components, SYCP2 and SYCP3, were increased in *Plk1* cKO spermatocytes, suggesting a defect during meiotic prophase. We also assessed the localization of PLK1 on chromatin spread preparations and confirmed the absence of PLK1 signal normally seen along chromosome axes and kinetochores in *Plk1* cKO spermatocytes (Supplemental Figure S1).

PLK1 is required for efficient SC lateral element disassembly and progression through meiosis I

We assessed the first wave of spermatogenesis in juvenile mice to determine more closely what stage of spermatogenesis is affected. We measured the testis weight of juvenile control and *Plk1* cKO littermates at ages that represent different stages of meiotic progression, spanning 15–16 dpp (mid-prophase), 18–19 dpp (late prophase), and 21–25 dpp (meiosis I and II; Supplemental Figure S2A). Testis weight was comparable between control and *Plk1* cKO mice at the first two ages, but a significant difference in weight was observed between 21 and 25 dpp, suggesting that primary spermatocytes are undergoing apoptosis during the transition between prophase and metaphase I.

We recently determined that the terminal phenotype for *Plk1* cKO spermatocytes was due to centrosome separation failure (Alfaro *et al.*, 2021; Wellard *et al.*, 2021). Nevertheless, PLK1 is also present within the nucleus during meiotic prophase in mouse spermatocytes and has been linked with a role in SC disassembly (Ishiguro *et al.*, 2011; Jordan *et al.*, 2012). Therefore, we next assessed the substages of meiotic prophase using chromatin spread preparations and staining for SC components, SYCP1, SYCP2, and SYCP3 (Figure 1C and Supplemental Figure S2B). At 14, 16, 18, and 20 dpp, we did not observe significant differences in the distribution of meiotic stages between control and *Plk1* cKO spermatocytes (Supplemental Figure S2C). Chromosome synapsis and formation of the sex body appeared normal in the *Plk1* cKO spermatocytes (Supplemental Figure S2B). However, we did observe SC disassembly defects in the *Plk1* cKO (Figure 1, C–G, and Supplemental Figure S2B). Most strikingly, the lateral elements of the SC, SYCP2 and SYCP3, were retained along chromosome arms at diakinesis (Figure 1, C–E). This contrasts with spermatocyte chromatin spreads from littermate controls, where SYCP2 and SYCP3 are predominantly retained on the kinetochore at diakinesis but disassembled from chromosome arms, as previously reported (Parra *et al.*, 2009; Bisig *et al.*, 2012; Qiao *et al.*, 2012). Furthermore, intense SYCP2 and SYCP3 polycomplex signals were observed in the majority of chromatin spread preparations, indicating aberrancies in SC disassembly and SC protein degradation (Figure 1, F and G).

These observations were consistent with our assessment of protein levels in STA-PUT isolated prophase spermatocytes, where SYCP2 and SYCP3 levels where higher in *Plk1* cKO spermatocytes compared with controls (Figure 1B). We also assessed changes in protein levels in germ cell extracts isolated during the first wave of spermatogenesis (Supplemental Figure 2, D–G). Control and *Plk1* cKO spermatocytes progress to late pachynema with similar timing according to accumulation of histone variant, H1T, which is present on chromatin from late pachynema onward (Lin *et al.*, 2004). This complements the similar distribution of meiotic prophase stages observed from 14 to 20 dpp in control and *Plk1* cKO mice during the first wave of spermatogenesis (Supplemental Figure S2C). Regarding SC components, protein extracts from the *Plk1* cKO displayed higher levels of SYCP1 and SYCP2 during the later stages of the first wave of spermatogenesis, particularly at 18 dpp. Taken together with the cytological analyses, these observations suggest that SC processes leading up to late prophase are occurring with normal kinetics in the *Plk1* cKO, but the transition from diplonema to diakinesis stages is perturbed.

It has been reported that PLK1 is required for activation of Aurora B kinase in mitotic cells (Chu *et al.*, 2011; Lee *et al.*, 2021). We previously showed that Aurora B kinase and the germ cell–specific Aurora C kinase are required for efficient disassembly of the SC lateral elements during mouse and human spermatogenesis (Wellard

et al., 2020). Both Aurora B and Aurora C have a common interaction partner, INCENP, which localizes to the SC during pachynema and then redistributes to pericentromeric heterochromatin by diplonema (Parra *et al.*, 2003, 2009). INCENP is reported to be required for appropriate recruitment and activation of Aurora B and Aurora C, which in turn phosphorylates the C terminus of INCENP (Tang *et al.*, 2006; Salimian *et al.*, 2011). Therefore, we assessed whether the localization of phosphorylated INCENP (p-INCENP) was affected by the absence of PLK1 in spermatocytes (Supplemental Figure S3A). p-INCENP foci were evident on diplotene-stage chromatin spreads from control and *Plk1* cKO spermatocytes. By diakinesis, p-INCENP predominantly localizes to pericentromeric heterochromatin in control spermatocytes. In contrast, p-INCENP localizes along chromosome axes, colocalizing with SYCP3, which is abnormally retained in *Plk1* cKO spermatocytes at diakinesis. These observations suggest that Aurora B/C kinase activity is not affected by the absence of PLK1, but their localization is perturbed.

PLK1 becomes enriched at the kinetochores during the transition from diplonema to diakinesis (Jordan *et al.*, 2012; Kim *et al.*, 2015a). Localization of PLK1 to the kinetochore was reported to be dependent on MEIKIN, a meiosis-specific protein required for sister kinetochore mono-orientation and centromeric cohesion (Kim *et al.*, 2015a). In contrast, from analysis of *Plk1* cKO spermatocytes at diakinesis, we found that PLK1 is not required for MEIKIN localization to the kinetochore during meiotic prophase (Supplemental Figure S3B). MEIKIN has been proposed to be the functional homologue of Moa1 and Spo13 from *Schizosaccharomyces pombe* and *Saccharomyces cerevisiae*, respectively (Kim *et al.*, 2015a). It has not been reported whether mutation of *Plk1* homologues in these two species affects localization of Moa1 or Spo13. However, it is known that expression of the budding yeast PLK, Cdc5, influences Spo13 protein levels, as overexpression of Cdc5 caused premature Spo13 degradation, and depletion of Cdc5 results in Spo13 stabilization during meiosis (Attner *et al.*, 2013).

Conditional mutation of Plk1 results in increased RPA foci and reduced RAD51/DMC1 foci during zygonema

Although mutation of *Plk1* does not affect the progression through the early stages of meiotic prophase, it has been demonstrated that PLK1 is important for DNA recombination events during meiosis in other model organisms (Clyne *et al.*, 2003; Sourirajan and Lichten, 2008; Matos *et al.*, 2011; Argunhan *et al.*, 2017; Nadarajan *et al.*, 2017; Wild *et al.*, 2019). Therefore, we assessed markers of different stages of meiotic recombination on prophase spermatocyte chromatin spread preparations.

We first assessed IHO1, which is essential for the formation of DSBs during meiosis (Stanzione *et al.*, 2016). Based on the localization of IHO1 during zygonema, we did not observe any difference between the control and *Plk1* cKO (Supplemental Figure S4).

To assess early response to SPO11-induced DSBs, we analyzed the localization of components of the RPA and MEIOB-SPATA22 complexes, which both independently bind to the 3′ ssDNA overhangs that are produced when meiotic DSBs undergo 5′ single-strand resection (Luo *et al.*, 2013; Shi *et al.*, 2019). We determined that *Plk1* cKO spermatocytes contained 25% more axial RPA2 foci compared with control spermatocytes at zygonema (Figure 2, A and B). In contrast, we did not observe a change in axial SPATA22 foci numbers in *Plk1* cKO spermatocytes compared with control spermatocytes at zygonema (Figure 2, C and D). We also assessed protein levels of RPA components, RPA1 and RPA2, and SPATA22 during the first wave of spermatogenesis (Figure 2E). No significant difference in protein levels between control and *Plk1* cKO was

observed, indicating that the increased RPA2 foci in *Plk1* cKO spermatocytes are not due to a change in expression level. Together, the data suggests that *Plk1* cKO spermatocytes fail to efficiently process RPA bound ssDNA at break sites, but do not influence MEIOB-SPATA22 processes.

To facilitate strand exchange between homologues, RPA on the 3′ ssDNA overhangs is displaced by the DNA recombinases RAD51 and DMC1 (Hunter and Kleckner, 2001; Sansam and Pezza, 2015). We observed significantly less RAD51 and DMC1 foci localized along the SYCP3 axes during late zygonema in the *Plk1* cKO spermatocytes compared with controls (Figure 2, F–I). Mean RAD51 and DMC1 foci numbers at late zygonema were 93.9 and 85.1, respectively, for *Plk1* cKO spermatocytes, compared with 126.3 and 133.2, respectively, for control spermatocytes. As repair of DSBs via HR is being completed, the numbers of RAD51 and DMC1 foci reduce, which is evident by pachynema. Despite the *Plk1* cKO having an ~25% reduction in RAD51 foci and an ~35% reduction in DMC1 foci at late zygonema, by early pachynema the numbers of RAD51 and DMC1 foci on autosomal pairs are similar between *Plk1* cKO and control mice (Figure 2, G and I). The reduced RAD51 foci during zygonema was not due to a reduction in protein expression, as we did not observe a significant decrease in RAD51 protein levels during the first wave of spermatogenesis via Western blot analysis (Figure 2, J and K). In fact, there may be an increase in RAD51 protein levels in *Plk1* cKO spermatocytes compared with control at 14 dpp. In a previous study, it was shown that PLK1 phosphorylates the serine 14 residue of RAD51 (pRAD51(ser14)) in human cell lines (HeLa, U20S, and HEK cell lines), and inability to phosphorylate this residue results in diminished foci formation upon DNA damage (Yata *et al.*, 2012). The researchers of this study developed an antibody to specifically detect pRAD51(ser14). The amino acid sequence used to create the pRAD51(ser14) is conserved in mouse, with the exception of one amino acid (asparagine in human vs. serine in mouse at position 10). We reasoned that mutation of *Plk1* during spermatogenesis may lead to reduced pRAD51(ser14) levels, which may be responsible for the reduced RAD51 foci on SYCP3 axes during late zygonema. Unfortunately, using the pRAD51(ser14) antibody, we did not detect a specific band via Western blot or foci on chromatin spreads and, thus, were unable to assess levels of pRAD51(ser14).

Taken together, conditional mutation of *Plk1* in spermatocytes results in disruption of meiotic DDR events, specifically in the context of RPA, DMC1, and RAD51 foci formation during zygonema. However, this defect does not cause meiotic arrest and *Plk1* cKO spermatocytes progress beyond the pachytene stage.

Conditional mutation of Plk1 results in increased class I crossover events

We further assessed DNA damage repair by examining the immunostaining pattern of phospho-histone H2A.X (γH2AX[ser139]). During leptonema and early zygonema γH2AX(ser139) marks most of the chromatin. As DNA repair and synapsis occur, during later stages of zygonema, the γH2AX(ser139) positive regions diminish. By pachynema γH2AX(ser139) is predominant at the X-Y chromosome pair, which undergoes specialized DDR and repair processes known as meiotic sex chromosome inactivation that persists into diplonema (Chicheportiche *et al.*, 2007). In addition to the X-Y chromosome pair, γH2AX(ser139) is also maintained at ongoing recombination sites on the autosomes during pachynema (Bondarieva *et al.*, 2020). We determined that *Plk1* cKO spermatocytes contain 21% more autosomal γH2AX(ser139) foci than control spermatocytes

(Figure 3, A and B). This observation implies that *Plk1* cKO spermatocytes take longer to repair DSBs than control spermatocytes. Moreover, there may be an altered recombination landscape in *Plk1* cKO spermatocytes, which could change the distribution of crossovers and noncrossovers.

To address whether mutation of *Plk1* in spermatocytes causes changes in class I crossover frequency, we assessed the number of CDK2 and MLH1 foci along SYCP3 axes at midpachynema. Control spermatocytes had averages of 19.5 and 23.1 crossover-associated CDK2 and MLH1 foci, respectively (Figure 3, C–F), whereas *Plk1* cKO spermatocytes had higher averages of crossover-associated CDK2 and MLH1 foci, 23.1 and 25, respectively. The higher number of CDK2 foci in the *Plk1* cKO compared with control was not coupled with a significant difference in CDK2 protein levels at any stage of the first wave of spermatogenesis (Figure 3G). In addition, SYCP3 axes that contained more than one MLH1 focus showed no alteration in the spacing between crossovers (Supplemental Figure S5, A and B). Nevertheless, the higher levels of CDK2 and MLH1 crossover foci observed in *Plk1* cKO spermatocytes compared with controls suggests that PLK1 is required to modulate class I crossover frequency.

Conditional mutation of Plk1 results in increased class II crossover events

The MUS81-EME1 resolvase is responsible for 5–10% of crossovers during spermatogenesis, and is classified as the class II crossover pathway (Holloway *et al.*, 2011). EME1 protein levels during the first wave of spermatogenesis were similar when comparing control and *Plk1* cKO (Figure 3G). To date, antibodies applicable for spermatocyte chromatin spread assessment of the MUS81-EME1 complex are not available. However, it is known that in the absence of the class I crossover pathway, class II crossover events can be assessed by counting how many homologues are linked via chiasma at the diakinesis stage, which are essential for bivalent formation (Holloway *et al.*, 2008, 2011). Therefore, we ablated the class I crossover pathway using an *Mlh3* knockout allele (Lipkin *et al.*, 2002). To observe bivalent formation, we treated spermatocytes isolated from 20 dpp mouse testes with the phosphatase inhibitor okadaic acid (OA), which stimulates midprophase spermatocytes to undergo SC disassembly, condense their chromosomes, and reach diakinesis (Wiltshire *et al.*, 1995; Sun and Handel, 2008). We assessed the number of bivalents in spermatocytes isolated from control, *Plk1* cKO, *Mlh3* KO, and *Plk1* cKO; *Mlh3* KO compound mutant mice. The control and *Plk1* cKO displayed similar numbers of bivalents, averaging 20 per spermatocyte (Figure 4, A–C). In contrast, the *Mlh3* KO spermatocytes had an average of two bivalents, which is expected based on the knowledge that the class II pathway is responsible for 5–10% of crossovers during spermatogenesis. Spermatocytes obtained from the *Plk1* cKO; *Mlh3* KO compound mutants had an average of four bivalents per spermatocyte, indicating that the absence of PLK1 during meiotic prophase increases the number of class II crossovers. To ensure that these results were not an artifact of varying populations of prophase substages in the testes of control and mutant mice, we counted the distribution of prophase substages in chromosome spreads immunolabeled against SYCP3 and SYCP1 in spermatocytes treated with a vehicle control (ethanol), or OA. No differences in prophase substage distribution were detected among the mice, and OA stimulated progression to diakinesis to a similar degree in any mouse (Figure 4, D and E). Conditional mutation of *Plk1* therefore influences both the class I and class II crossover formation pathways.
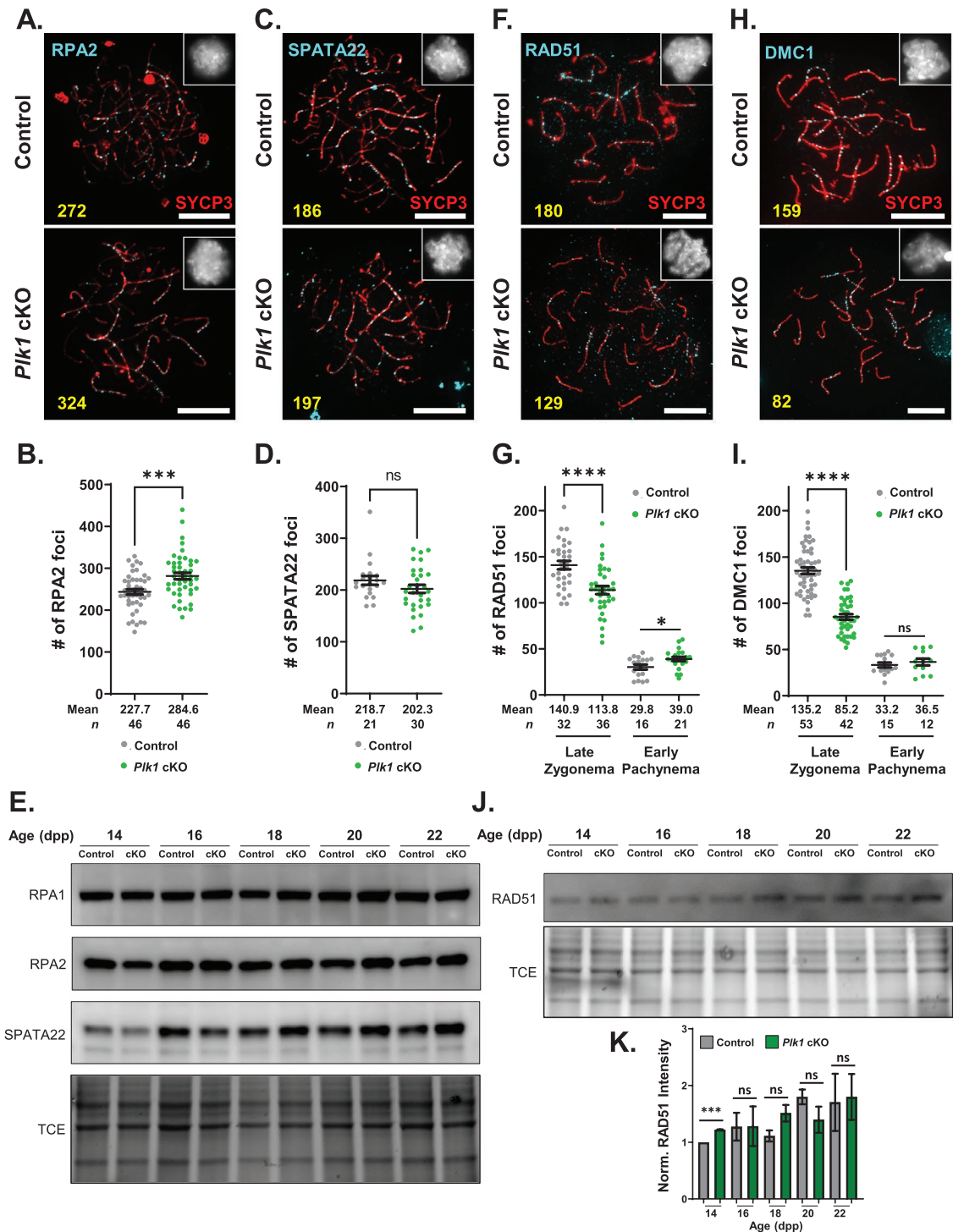
FIGURE 2: Deletion of *Plk1* in mouse spermatocytes results in abnormal early DNA damage repair processes.
(A) Representative chromatin spread preparations of zygotene-stage spermatocytes from control and *Plk1* cKO mice immunolabeled with SYCP3 (red) and RPA2 (cyan), and stained with DAPI (white inset). Scale bars = 10 μm.
(B) Quantification of RPA2 foci numbers at zygonema from three biological replicates in control (46 cells assessed) and *Plk1* cKO (46 cells assessed) spermatocytes. Error bars show mean ± SEM. *P* value (two-tailed Student's *t* test) comparing *Plk1* cKO to the control is indicated by ***, *P* < 0.001. (C) Representative chromatin spread preparations of zygotene-stage spermatocytes from control and *Plk1* cKO mice immunolabeled with SYCP3 (red) and SPATA22 (cyan), and stained with DAPI (white inset). Scale bars = 10 μm. (D) Quantification of SPATA22 foci from three biological replicates at zygonema in control (21 cells assessed) and *Plk1* cKO (30 cells assessed) spermatocytes. Error bars show mean ± SEM. *P* value (two-tailed Student's *t* test) comparing *Plk1* cKO to the control is indicated by ns (not significant). (E) Western blot analysis of RPA1, RPA2, and SPATA22 in control and *Plk1* cKO spermatocytes isolated from whole testis extracts from 14 to 22 dpp. Total protein stained with 2,2,2-trichloroethanol (TCE) to display protein loading. (F) Representative chromatin spread preparations of zygotene-stage spermatocytes from control and *Plk1* cKO mice

DISCUSSION

This study demonstrates that PLK1 influences several events during DNA damage repair and crossover formation during spermatogenesis (Figure 5A). Male *Plk1* cKO mice exhibit severe meiotic aberrancies and are infertile due to failed centrosome maturation and separation (Wellard *et al.*, 2021). Despite the cell cycle arrest we observe during the first meiotic division, we were able to assess the efficacy of DNA damage repair during meiotic prophase in mice undergoing the first wave of spermatogenesis. We observed increased levels of RPA2 foci and a concomitant decrease in single-end invasion intermediates, RAD51 and DMC1, during zygonema in *Plk1* cKO spermatocytes. Moreover, deletion of *Plk1* results in increased class I and class II crossover intermediates. We also observed perturbations to SC disassembly in *Plk1* cKO spermatocytes, where axial components persist into diakinesis (Figure 5B). These data indicate that PLK1 regulates crossover formation, and may link DNA damage repair with SC disassembly, in a cross-regulatory manner.

Roles for PLK1 in response to and repair of DSBs

PLK1 phosphorylates RAD51 (serine 14) during HR in mitotic cells (Yata *et al.*, 2012). This modification leads to further phosphorylation by casein kinase 2 (CK2), which facilitates the localization of RAD51 to DNA damage sites through interaction with NBS1, a component of the MRE11-RAD50-NBS1 (MRN) complex (Yata *et al.*, 2012). Interestingly, PLK1-dependent phosphorylation of MRE11 also results in further phosphorylation by CK2 (Li *et al.*, 2017). The dual phosphorylation by PLK1 and CK2 on MRE11 inhibits loading of the MRN complex to sites of DNA damage, which may allow downstream DNA repair proteins, such as RAD51 and DMC1, to have access and repair damaged DNA (Li *et al.*, 2017). The increased RPA2 foci numbers and decreased RAD51/DMC1 foci numbers observed in *Plk1* cKO zygotene-stage spermatocytes indicates that PLK1 is required for efficient transition from DNA damage detection to DNA damage repair during meiosis, which aligns well to its known functions in somatic cells, detailed above. Furthermore, the numbers of RAD51/DMC1 foci in *Plk1* cKO spermatocytes by early pachynema is similar to control spermatocytes. This observation suggests that rather than a reduction in RAD51/DMC1 foci number per se, abrogating PLK1 function results in a delay in DSB repair and recombination processes.

During meiosis, both RAD51 and DMC1 affect DNA damage repair and crossover formation, but how these proteins function together to promote strand exchange on the homologous chromosome remains an active area of research (Crickard and Greene, 2018). Studies have shown that RAD51 and DMC1 interact with unique binding partners, but still colocalize and form protein filaments in a side-by-side configuration at 3' ssDNA overhangs (Sheridan and Bishop, 2006; Brown *et al.*, 2015). Moreover, it has been suggested that cross-talk between binding partners on RAD51 and DMC1 could influence the stability of the nucleofilament (Crickard *et al.*, 2018). Posttranslational modifications on RAD51 and DMC1 that modulate the binding of cofactors could therefore have profound influences on DNA repair efficiency during meiosis. Determining the phosphostatus of RAD51 and DMC1 and other key repair factors during meiotic DNA damage repair in control and *Plk1* cKO mice will be necessary to further elucidate the mechanisms by which strand exchange and D-loop formation are regulated during meiosis. For instance, the breast cancer gene BRCA1, which is required to promote exchange of RPA with RAD51 in somatic cells during DSB repair, is also phosphorylated by PLK1 and is likely to be another key factor being regulated by PLK1 during meiosis (Chabalier-Taste *et al.*, 2016).

Increased levels of class I and class II crossover intermediates

Our observation that class I and class II crossover intermediates are increased in *Plk1* cKO spermatocytes aligns with work conducted in budding yeast, with some exceptions. The budding yeast PLK, Cdc5, is necessary and sufficient for the resolution of crossovers in meiosis (Clyne *et al.*, 2003; Sourirajan and Lichten, 2008). Cells lacking Cdc5 accumulate joint molecules, as do mouse spermatocytes lacking PLK1. However, Cdc5 deficiency results in reduced numbers of crossovers while maintaining their levels of noncrossovers (Allers and Lichten, 2001; Clyne *et al.*, 2003; Sourirajan and Lichten, 2008), whereas *Plk1* cKO mouse spermatocytes form equivalent numbers of bivalents compared with control mice (Figure 4, A–C), suggesting that crossover formation is completed, albeit with increased numbers compared with controls. These differences may be attributed to there being a more complex network of crossover assurance and interference in mammals, which must ensure crossovers are formed over a much larger genetic distance (Broman *et al.*, 2002). A recent study assessing mitotically dividing human cells demonstrated that PLK1 enhances the BLM-TOP3A-RMI1-RMI2 (BTR) -mediated dissolution of recombination intermediates late during the G2-M transition, which suppresses crossover recombination events (Balbo Pogliano *et al.*, 2022). This work aligns well with our observations, as we see a general increase in crossover intermediates. In future work, it would be interesting to determine whether the same relationship between PLK1 and BTR exists during mammalian meiosis.

An important next step is to determine what are the PLK1 phosphotargets that ensure crossover resolution. Cdc5 has been shown to regulate the activity of the class II resolvase Mus81-Mms4

immunolabeled with SYCP3 (red) and RAD51 (cyan), and stained with DAPI (white inset). Scale bars = 10 μm. (G) Quantification of RAD51 foci from three biological replicates at late zygonema and early pachynema in control (32 zygonema and 16 pachynema cells assessed) and *Plk1* cKO (36 zygonema and 21 pachynema cells assessed) spermatocytes. Error bars show mean ± SEM. *P* values (two-tailed Student's *t* test) comparing *Plk1* cKO to the control are indicated by ****, *P* < 0.0001. (H) Representative chromatin spread preparations of zygotene-stage spermatocytes from control and *Plk1* cKO mice immunolabeled with SYCP3 (red) and DMC1 (cyan), and stained with DAPI (white inset). Scale bars = 10 μm. (I) Quantification of DMC1 foci from three biological replicates at late zygonema and early pachynema in control (53 zygonema and 15 pachynema cells assessed) and *Plk1* cKO (42 zygonema and 12 pachynema cells assessed) spermatocytes. Error bars show mean ± SEM. *P* values (two-tailed Student's *t* test) comparing *Plk1* cKO to the control are indicated by ****, *P* < 0.0001. (J) Western blot analysis of RAD51 in control and *Plk1* cKO spermatocytes isolated from whole testis extracts from 14 to 22 dpp. Total protein stained with 2,2,2-TCE to display protein loading. (K) Quantification of relative band intensities for RAD51 from three independent Western blots. Error bars show mean ± SEM. *P* values (paired two-tailed Student's *t* test) comparing *Plk1* cKO to the control are indicated by ***, *P* < 0.001 or ns (not significant).
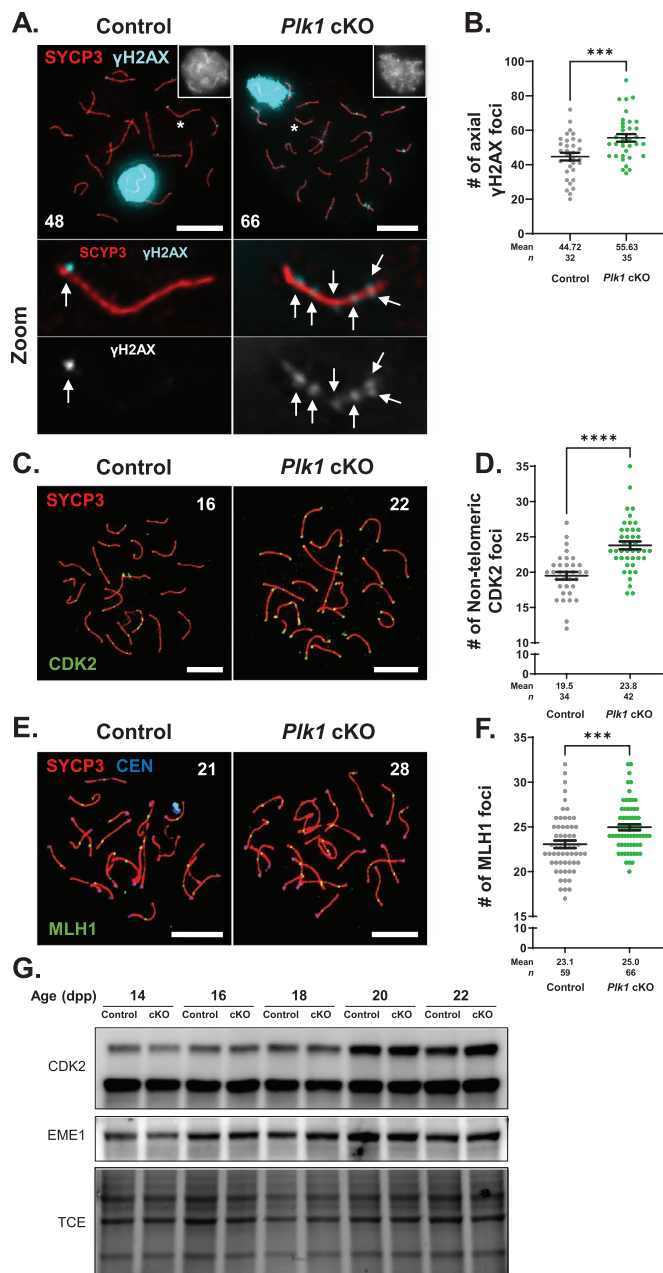
FIGURE 3: Deletion of *Plk1* in mouse spermatocytes results in elevated numbers of class I crossover intermediate markers.
(A) Representative chromatin spread preparations of pachytene stage spermatocytes from control and *Plk1* cKO mice immunolabeled with SYCP3 (red) and γH2AX (cyan), and stained with DAPI (white inset). The γH2AX signal intensity is intentionally overblown to visualize recombination node staining. White asterisk denotes chromosome axis used in the optical zoom panels which show SYCP3 (red) and γH2AX (cyan/white) immunolabeling. Scale bars = 10 μm. (B) Quantification of γH2AX foci from three biological replicates at pachynema in control (32 cells assessed) and *Plk1* cKO (35 cells assessed) spermatocytes. Error bars show mean ± SEM. *P* values (two-tailed Student's *t* test) comparing *Plk1* cKO to the control are indicated by ***, *P* < 0.001. (C) Representative chromatin spread preparations of pachynema spermatocytes from control and *Plk1* cKO mice immunolabeled with SYCP3 (red) and CDK2 (green). Scale bars = 10 μm. (D) Quantification of nontelomeric CDK2 foci at pachynema in control (34 cells assessed) and *Plk1* cKO (42 cells assessed) spermatocytes. Telomere localized CDK2 foci are excluded from this analysis. Error bars show mean ± SEM. *P* values (two-tailed Student's

t test) comparing *Plk1* cKO to the control are indicated by ****, *P* < 0.0001. (E) Representative chromatin spread preparations of pachynema spermatocytes from control and *Plk1* cKO mice immunolabeled with centromere (CEN; blue), SYCP3 (red), and MLH1 (green). Scale bars = 10 μm. (F) Quantification of MLH1 foci numbers at pachynema in control (59 cells assessed) and *Plk1* cKO (66 cells assessed) spermatocytes. Error bars show mean ± SEM. *P* values (two-tailed Student's *t* test) comparing *Plk1* cKO to the control are indicated by ***, *P* < 0.001. (G) Western blot analysis of CDK2 and EME1 in control and *Plk1* cKO spermatocytes isolated from whole testis extracts from 14 to 22 dpp. Total protein stained with 2,2,2-trichloroethanol (TCE) to display protein loading.

(MUS81-EME1) by phosphorylating Mms4 (de los Santos *et al.*, 2003; Matos *et al.*, 2011). This activity is conserved in mammals, where PLK1 activates MUS81-EME1 by phosphorylating EME1 during mitosis (Svendsen *et al.*, 2009; Wyatt *et al.*, 2013). Moreover, Cdc5 directly interacts with MutLγ-Exo1 complexes at class I recombination sites (Sanchez *et al.*, 2020). Therefore, Cdc5 has been shown to associate with and regulate both class I and class II crossovers, but whether these crossover-associated protein interactions are conserved in mammals remains to be shown. Identification of the phosphoproteomes from purified prophase spermatocytes in control and *Plk1* cKO mice would assist in determining the mechanism through which PLK1 influences crossover formation in mammals.

Linking crossover recombination with SC disassembly
Crossover formation during meiosis takes place in the context of chromosome synapsis, mediated by the SC. The SC acts as a signaling hub to link events occurring at recombination nodes to alterations in chromatin morphology throughout the chromosome (Cahoon and Hawley, 2016). The best example of interplay between the SC and crossover formation has been determined in *C. elegans*, where defects in crossover formation result in a cell cycle delay mediated by the cell cycle kinase CHK-2 (Kim *et al.*, 2015b). *C. elegans* PLK-1 and PLK-2 paralogues are recruited to pairing centers on the SC and fulfill a similar role by mediating a cell cycle delay when chromosomes fail to synapse (Harper *et al.*, 2011; Labella *et al.*, 2011). In *C. elegans*, PLKs play an early role during crossover formation by regulating DSB formation through phosphorylation of SC components. The phosphorylation of SYP-4 by PLK-1/2 changes the SC from a more dynamic to a less dynamic state, reducing the ability for further DSBs to form (Machovina *et al.*, 2016; Nadarajan *et al.*, 2017). While PLKs seem to play a more critical role in the early events of DNA damage formation and repair during meiosis in worms than in mice, the localization of PLK-1 and PLK-2 to the SC and pairing centers is important for regulating the timing of SC disassembly, which is similar to what we observe in this study.

The localization of PLKs to the SC is not restricted to *C. elegans*. PLK1 localizes to the SC and is capable of directly phosphorylating the SC proteins SYCP1 and TEX12 (Jordan *et al.*, 2012). Additionally, inhibition of PLK activity resulted in SC disassembly defects (Ishiguro *et al.*, 2011; Jordan *et al.*, 2012), which were similar to what we have observed in *Plk1* cKO spermatocytes (Figure 1, C–G). These observations raise the intriguing hypothesis that PLK1 may coordinate the initiation of SC disassembly with the completion of crossover formation. However, due to the cell cycle arrest at metaphase I that occurs in *Plk1* cKO spermatocytes, we are unable to assess whether the defects observed during crossover formation and SC disassembly would contribute to chromosome missegregation and aneuploidy (Wellard *et al.*, 2021).

FIGURE 4: The number of class II crossover repair intermediates is increased in *Plk1* cKO mice. (A) Representative chromatin spread preparations of spermatocytes at diakinesis following a 5-h okadaic acid (OA) treatment from control, *Plk1* cKO, *Mlh3* KO, and *Plk1; Mlh3* double KO (dKO) mice immunolabeled with centromeres (CEN; magenta) and stained with DAPI (green). Scale bars = 10 µm. Optical zooms highlight bivalent and univalent structures observed following OA treatment and are indicated with white asterisks. (B) Optical zooms of individual bivalents labeled in A with arrow and unique roman numeral (i from control; ii from *Plk1* cKO; iii from *Mlh3* KO; iv, v, and vi from *Plk1; Mlh3* dKO). Each bivalent is immunolabeled with SYCP3 (green) and centromeres (magenta). The dashed outline represents the DNA imaged via DAPI. Scale bars = 2 µm. (C) The number of bivalents observed per diakinesis spermatocyte following OA treatment for control, *Plk1* cKO, *Mlh3* KO, and *Plk1; Mlh3* dKO was quantified in 30 spermatocytes from three biological replicates. Error bars show mean ± SEM. *P* values (two-tailed Student's *t* test) comparing mutant mice to controls are indicated. (D, E) Prophase substages were quantified from 20 dpp control, *Plk1* cKO, *Mlh3* KO, and *Plk1; Mlh3* dKO mice from which spermatocytes were treated with either a vehicle control (ethanol, EtOH; D), or OA (E). At least 100 cells were counted from three biological replicates, and each count was conducted twice. Error bars show mean ± SEM. *P* values (two-tailed Student's *t* test) comparing mutant mice to controls were not significant.

Phosphorylation of many SC and axis proteins during the first wave of spermatogenesis has been reported, and these modifications occur in a cell cycle–dependent manner (Fukuda *et al.*, 2012). It is likely that PLK1 together with other cell cycle kinases, such as CDKs, and Aurora B and C kinases, regulate SC dynamics and DNA repair in a cooperative and coordinated manner. For instance, Aurora B and Aurora C kinases are required for lateral element disassembly (Sun and Handel, 2008; Wellard *et al.*, 2020), and we show here that PLK1 is required for normal localization of its anchoring interaction partner and substrate, INCENP
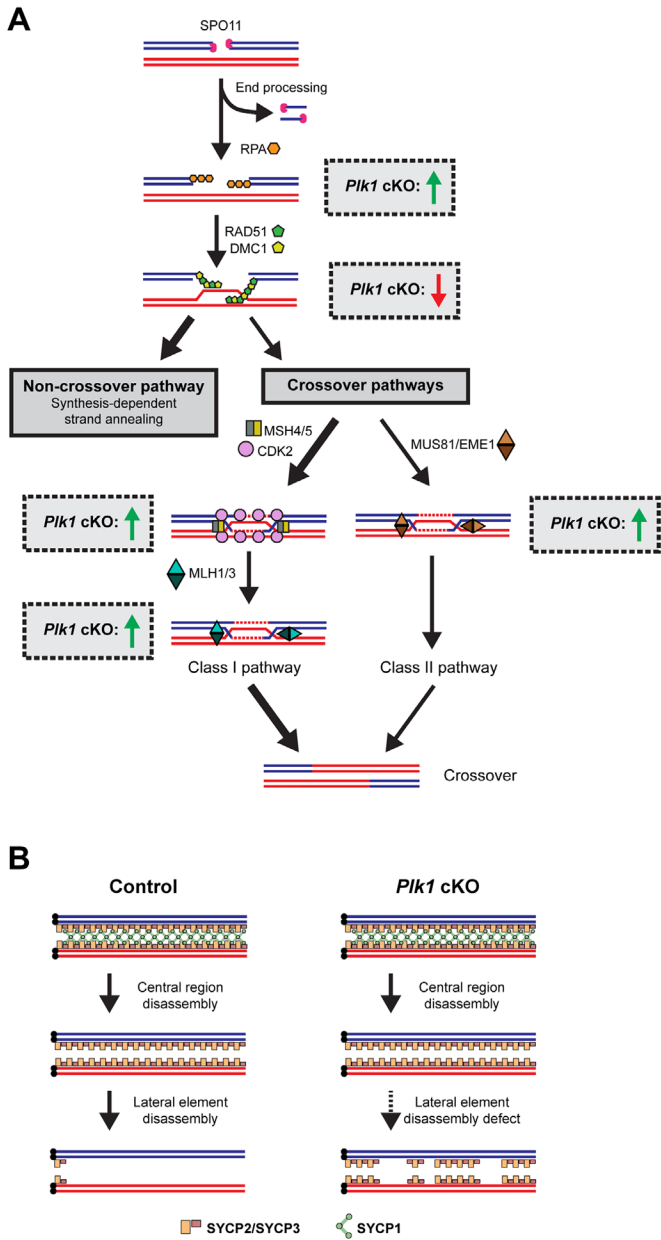
FIGURE 5: Model for the role of PLK1 during meiotic DNA damage repair, crossover formation, and SC lateral element disassembly in mouse spermatocytes. (A) Crossover formation during meiosis relies on the complex regulation of DNA damage repair proteins which act to ensure that each homologue pair generates a physical linkage during meiotic prophase. Assessment of components required for sequential steps during the DNA damage repair and crossover formation pathways implies that PLK1 is involved in regulating several key steps. First, PLK1 may influence early DNA damage repair by regulating the localization of single-strand binding proteins such as RPA (increased in *Plk1* cKO spermatocytes) and RAD51/DMC1 (decreased in *Plk1* cKO spermatocytes). Later, PLK1 may influence the resolution of double holiday junctions, as *Plk1* cKO spermatocytes containing increased numbers of both class I and class II recombination intermediates are observed. (B) Disassembly of central region components of the SC initiates during the transition from pachynema to diplonema. Lateral element components of the SC are then disassembled during the transition from diplonema to diakinesis. Based on the assessment of *Plk1* cKO spermatocytes, PLK1 is required for efficient disassembly and degradation of lateral element

(Supplemental Figure S3A). However, further work is needed to determine how these cell cycle kinases work together during mammalian meiosis.

In conclusion, we show that PLK1 is important for regulating DSB repair and SC disassembly during mouse spermatogenesis. Incorporation of the *Plk1* cKO approach in a F1 hybrid genetic background would enable a genome-wide assessment of changes to the recombination landscape. Furthermore, determining PLK1 interactors and substrates will contribute to further defining the roles for PLK1 in meiotic recombination and SC biogenesis.

MATERIALS AND METHODS
Request a protocol through *Bio-protocol*.

Ethics statement
All mice were bred at Johns Hopkins University (JHU; Baltimore, MD) in accordance with the National Institutes of Health (NIH) and U.S. Department of Agriculture criteria and protocols for their care and use were approved by the Institutional Animal Care and Use Committees of JHU.

Mice
mESC clone HEPD0663_7_E04 (C57BL/6N-A/a genetic background) bearing a "knockout first" allele of *Plk1* (*Plk1^{tm1a(EUCOMM)Hmgu}*) were acquired from the Knockout Mouse Project as previously described (Little and Jordan, 2020; Wellard *et al.*, 2021).

Chimeras were obtained by microinjection of HEPD0663_7_E04 mESCs into C57BL/6JN blastocyst-stage mouse embryos and assessed for germline transmission. Heterozygous progeny were bred with a C57BL/6J Flp recombinase deleter strain (B6.129S4-*Gt(ROSA)26Sor^{tm1(FLP1)Dym}*/RainJ, JAX) to remove the *SA-LacZ* and *Neo* selection cassette and produce the floxed exon 4 (designated *Plk1 flox*).

To produce heterozygous offspring for the deleted exon 4 (designated *Plk1 del*), heterozygous *Plk1 flox* males were mated to *Sox2-Cre* C57BL/6J (B6.Cg-Tg(Sox2-cre)1Amc/J; JAX) mice.

Further, heterozygous *Plk1 del* mice were bred to mice harboring the Cre transgenes that are specifically expressed in germ cells; *Spo11-Cre* (C57BL/6-Tg Spo11-cre)1Rsw/PecoJ), which resulted in male progeny heterozygous for the *Plk1 del* allele and hemizygous for the germ cell–specific Cre transgene. These mice were bred to female homozygous *Plk1 flox* mice to derive *Plk1* cKO (*Plk1 flox/del*, Cre) and control (*Plk1 +/flox*) genotypes.

PCR genotyping
Primers used are described in Supplemental Table S1 and as previously described (Little and Jordan, 2020; Wellard *et al.*, 2021). PCR conditions: 90°C for 2 min; 35 cycles of 90°C for 20 s, 58°C, 72°C for 1 min. A final extension of 10 min at 72°C was used.

Histological analysis
Testes were fixed in Bouins fixative. Fixed tissues were embedded in paraffin and serial sections of 5-μm thickness were placed onto slides and stained with H&E.

components of the SC. SC disassembly is likely coordinated by the action of several cell cycle kinases including PLK1, CDK1, Aurora B, and Aurora C kinases (Sun and Handel, 2008; Ishiguro *et al.*, 2011; Jordan *et al.*, 2012; Cahoon and Hawley, 2016; Gao and Colaiácovo, 2018; Wellard *et al.*, 2020).

Mouse spermatocyte isolation and culturing conditions

Mixed mouse germ cell populations were isolated as described previously (Bellvé, 1993; La Salle et al., 2009). Midprophase-enriched spermatocytes were isolated from 14, 16, 18, 20, and 22 dpp mice, undergoing the semisynchronous first wave of spermatogenesis.

Enriched primary spermatocytes from adult mice were isolated using STA-PUT gravity sedimentation as previously described with minor adjustments (La Salle et al., 2009). A density gradient was created by flowing 550 ml of 4% bovine serum albumin (BSA) in Krebs-Ringer modified buffer (KRB) and 550 ml of 2% BSA in KRB into the 25 ml of cell suspension in 0.5% BSA in KRB. Cells were sedimented for 3 h before elution and fractionation into 12×75-mm glass culture tubes. Aliquots from each fraction were assessed to determine the purity of isolated primary spermatocytes, as identified from cell shape and size. Fractions containing abundant (90% pure) primary spermatocytes were pooled, counted, and centrifuged at $500 \times g$ to resuspend at a cell concentration of 2.5×10^6 cells/ml.

Mouse spermatocytes were cultured at 32°C in 5% CO_2 in HEPES (25 mM)-buffered MEMα culture medium (Sigma) supplemented with 25 mM NaHCO$_3$, 5% fetal bovine serum (Atlanta Biologicals), 10 mM sodium lactate, 59 µg/ml penicillin, and 100 µg/ml streptomycin. Spermatocytes were stimulated to undergo the G2/MI transition by a 4 µM OA (Sigma) treatment for 5 h, then assessed via chromatin spread preparation.

Protein analyses

For protein level analyses, proteins were extracted from germ cells using RIPA buffer (Santa Cruz) containing 1× protease inhibitor cocktail (Roche). Protein concentration was calculated using a Bicinchoninic acid (BCA) protein assay kit (Pierce). Lanes of 6%, 10%, 15%, and 4–15% gradient SDS polyacrylamide gels (Bio-Rad) were loaded with 20 µl of 1 mg/ml protein extract. Following protein separation via standard SDS–PAGE, proteins were transferred to polyvinylidene difluoride (PVDF) membranes using the Trans-Blot Turbo Western transfer system (Bio-Rad). Primary antibodies and dilution used are presented in Supplemental Table S2. At a 1:5000 dilution, goat anti-mouse (62-6520) and goat anti-rabbit (A10533) horseradish peroxidase–conjugated antibodies (Invitrogen) were used as secondary antibodies. The presence of antibodies on the PVDF membranes was detected via treatment with Pierce ECL Western blotting substrate (Thermo Scientific) and captured using the Syngene XR5 gel documentation system. Protein levels were assessed using Image J (NIH).

Chromatin spread analyses

Germ cell chromatin spreads were prepared as previously described (Jordan et al., 2012), or with some modifications. Briefly, germ cells were placed in 50% hypotonic buffer (30 mM Tris, 50 mM sucrose, 17 mM trisodium citrate dihydrate, 5 mM EDTA, 2.5 mM dithiothreitol) for 8 min. The cells were then resuspended in a second hypotonic buffer (1:1 of phosphate-buffered saline and 100 µM sucrose). The cell suspension was fixed using 1% paraformaldehyde on a glass slide for 1 h in a humid chamber. The slides were air dried for 1 h, washed in 0.4% Photo-Flo (Kodak) in H_2O overnight, and dried again for 30 min. The slides were immunolabeled immediately afterward. Primary antibodies and dilution used are presented in Supplemental Table S2. Secondary antibodies against human, rabbit, rat, mouse, and guinea pig IgG and conjugated to Alexa 350, 488, 568, or 633 (Life Technologies) were used at a dilution of 1:500.

Microscopy

Images from chromatin spread preparations were captured using a Zeiss CellObserver Z1 microscope linked to an ORCA-Flash 4.0 CMOS camera (Hamamatsu). Testis sections stained with H&E staining were captured using a Zeiss AxioImager A2 microscope linked to an AxioCam ERc5s camera, or Keyence BZ-X800 fluorescence microscope. Images were analyzed and processed using ZEN 2012 blue edition imaging software (Zeiss) or with BZ-X800 Viewer and Analyzer software (Keyence).

REFERENCES

Alfaro E, López-Jiménez P, González-Martínez J, Malumbres M, Suja JA, Gómez R (2021). PLK1 regulates centrosome migration and spindle dynamics in male mouse meiosis. EMBO Rep 22, e51030.

Allers T, Lichten M (2001). Differential timing and control of noncrossover and crossover recombination during meiosis. Cell 106, 47–57.

Anderson LK, Reeves A, Webb LM, Ashley T (1999). Distribution of crossing over on mouse synaptonemal complexes using immunofluorescent localization of MLH1 protein. Genetics 151, 1569–1579.

Argunhan B, Leung W-K, Afshar N, Terentyev Y, Subramanian VV, Murayama Y, Hochwagen A, Iwasaki H, Tsubouchi T, Tsubouchi H (2017). Fundamental cell cycle kinases collaborate to ensure timely destruction of the synaptonemal complex during meiosis. EMBO J 36, 2488–2509.

Attner MA, Miller MP, Ee L, Elkin SK, Amon A (2013). Polo kinase Cdc5 is a central regulator of meiosis I. Proc Natl Acad Sci USA 110, 14278–14283.

Balbo Pogliano C, Ceppi I, Giovannini S, Petroulaki V, Palmer N, Uliana F, Gatti M, Kasaciunaite K, Freire R, Seidel R, et al. (2022). The CDK1-TOPBP1-PLK1 axis regulates the Bloom's syndrome helicase BLM to suppress crossover recombination in somatic cells. Sci Adv 8, eabk0221.

Bellani MA, Romanienko PJ, Cairatti DA, Camerini-Otero RD (2005). SPO11 is required for sex-body formation, and Spo11 heterozygosity rescues the prophase arrest of Atm-/- spermatocytes. J Cell Sci 118, 3233–3245.

Bellvé AR (1993). Purification, culture, and fractionation of spermatogenic cells. Meth Enzymol 225, 84–113.

Bergerat A, de Massy B, Gadelle D, Varoutas PC, Nicolas A, Forterre P (1997). An atypical topoisomerase II from Archaea with implications for meiotic recombination. Nature 386, 414–417.

Bisig CG, Guiraldelli MF, Kouznetsova A, Scherthan H, Höög C, Dawson DS, Pezza RJ (2012). Synaptonemal complex components persist at centromeres and are required for homologous centromere pairing in mouse spermatocytes. PLoS Genet 8, e1002701.

Boddy MN, Gaillard P-HL, McDonald WH, Shanahan P, Yates JR, Russell P (2001). Mus81-Eme1 are essential components of a Holliday junction resolvase. Cell 107, 537–548.

Bolcun-Filas E, Handel MA (2018). Meiosis: the chromosomal foundation of reproduction. Biol Reprod 99, 112–126.

Bondarieva A, Raveendran K, Telychko V, Rao HBDP, Ravindranathan R, Zorzompokou C, Finsterbusch F, Dereli I, Papanikos F, Tränkner D, et al. (2020). Proline-rich protein PRR19 functions with cyclin-like CNTD1 to promote meiotic crossing over in mouse. Nat Commun 11, 3101.

Brandt JN, Hussey KA, Kim Y (2020). Spatial and temporal control of targeting Polo-like kinase during meiotic prophase. J Cell Biol 219, e202006094.

Broman KW, Rowe LB, Churchill GA, Paigen K (2002). Crossover interference in the mouse. Genetics 160, 1123–1131.

Brown MS, Grubb J, Zhang A, Rust MJ, Bishop DK (2015). Small Rad51 and Dmc1 complexes often co-occupy both ends of a meiotic DNA double strand break. PLoS Genet 11, e1005653.

Cahoon CK, Hawley RS (2016). Regulating the construction and demolition of the synaptonemal complex. Nat Struct Mol Biol 23, 369–377.

Chabalier-Taste C, Brichese L, Racca C, Canitrot Y, Calsou P, Larminat F (2016). Polo-like kinase 1 mediates BRCA1 phosphorylation and recruitment at DNA double-strand breaks. Oncotarget 7, 2269–2283.

Chicheportiche A, Bernardino-Sgherri J, de Massy B, Dutrillaux B (2007). Characterization of Spo11-dependent and independent phospho-H2AX foci during meiotic prophase I in the male mouse. J Cell Sci 120, 1733–1742.

Chu Y, Yao PY, Wang W, Wang D, Wang Z, Zhang L, Huang Y, Ke Y, Ding X, Yao X (2011). Aurora B kinase activation requires survivin priming phosphorylation by PLK1. J Mol Cell Biol 3, 260–267.

Clyne RK, Katis VL, Jessop L, Benjamin KR, Herskowitz I, Lichten M, Nasmyth K (2003). Polo-like kinase Cdc5 promotes chiasmata formation and cosegregation of sister centromeres at meiosis I. Nat Cell Biol 5, 480–485.

Cole F, Keeney S, Jasin M (2010). Evolutionary conservation of meiotic DSB proteins: more than just Spo11. Genes Dev 24, 1201–1207.

Costa Y, Cooke HJ (2007). Dissecting the mammalian synaptonemal complex using targeted mutations. Chromosome Res 15, 579–589.

Crickard JB, Greene EC (2018). The biochemistry of early meiotic recombination intermediates. Cell Cycle 17, 2520–2530.

Crickard JB, Kaniecki K, Kwon Y, Sung P, Greene EC (2018). Spontaneous self-segregation of Rad51 and Dmc1 DNA recombinases within mixed recombinase filaments. J Biol Chem 293, 4191–4200.

de Cárcer G, Manning G, Malumbres M (2011). From Plk1 to Plk5: functional evolution of polo-like kinases. Cell Cycle 10, 2255–2262.

de los Santos T, Hunter N, Lee C, Larkin B, Loidl J, Hollingsworth NM (2003). The Mus81/Mms4 endonuclease acts independently of double-Holliday junction resolution to promote a distinct subset of crossovers during meiosis in budding yeast. Genetics 164, 81–94.

Fraune J, Schramm S, Alsheimer M, Benavente R (2012). The mammalian synaptonemal complex: protein components, assembly and role in meiotic recombination. Exp Cell Res 318, 1340–1346.

Fukuda T, Pratto F, Schimenti JC, Turner JMA, Camerini-Otero RD, Höög C (2012). Phosphorylation of chromosome core components may serve as axis marks for the status of chromosomal events during mammalian meiosis. PLoS Genet 8, e1002485.

Gao J, Colaiácovo MP (2018). Zipping and unzipping: protein modifications regulating synaptonemal complex dynamics. Trends Genet 34, 232–245.

Harper NC, Rillo R, Jover-Gil S, Assaf ZJ, Bhalla N, Dernburg AF (2011). Pairing centers recruit a Polo-like kinase to orchestrate meiotic chromosome dynamics in C. elegans. Dev Cell 21, 934–947.

Holloway JK, Booth J, Edelmann W, McGowan CH, Cohen PE (2008). MUS81 generates a subset of MLH1-MLH3-independent crossovers in mammalian meiosis. PLoS Genet 4, e1000186.

Holloway JK, Mohan S, Balmus G, Sun X, Modzelewski A, Borst PL, Freire R, Weiss RS, Cohen PE (2011). Mammalian BTBD12 (SLX4) protects against genomic instability during mammalian spermatogenesis. PLoS Genet 7, e1002094.

Hunter N (2015). Meiotic recombination: the essence of heredity. Cold Spring Harb Perspect Biol 7, a016618.

Hunter N, Kleckner N (2001). The single-end invasion: an asymmetric intermediate at the double-strand break to double-holliday junction transition of meiotic recombination. Cell 106, 59–70.

Hwang G, Verver DE, Handel MA, Hamer G, Jordan PW (2018). Depletion of SMC5/6 sensitizes male germ cells to DNA damage. Mol Biol Cell 29, 3003–3016.

Ishiguro K, Kim J, Fujiyama-Nakamura S, Kato S, Watanabe Y (2011). A new meiosis-specific cohesin complex implicated in the cohesin code for homologous pairing. EMBO Rep 12, 267–275.

Jordan PW, Karppinen J, Handel MA (2012). Polo-like kinase is required for synaptonemal complex disassembly and phosphorylation in mouse spermatocytes. J Cell Sci 125, 5061–5072.

Keeney S, Giroux CN, Kleckner N (1997). Meiosis-specific DNA double-strand breaks are catalyzed by Spo11, a member of a widely conserved protein family. Cell 88, 375–384.

Kim J, Ishiguro K, Nambu A, Akiyoshi B, Yokobayashi S, Kagami A, Ishiguro T, Pendas AM, Takeda N, Sakakibara Y, et al. (2015a). Meikin is a conserved regulator of meiosis-I-specific kinetochore function. Nature 517, 466–471.

Kim Y, Kostow N, Dernburg AF (2015b). The chromosome axis mediates feedback control of CHK-2 to ensure crossover formation in C. elegans. Dev Cell 35, 247–261.

Kneitz B, Cohen PE, Avdievich E, Zhu L, Kane MF, Hou H, Kolodner RD, Kucherlapati R, Pollard JW, Edelmann W (2000). MutS homolog 4 localization to meiotic chromosomes is required for chromosome pairing during meiosis in male and female mice. Genes Dev 14, 1085–1097.

Labella S, Woglar A, Jantsch V, Zetka M (2011). Polo kinases establish links between meiotic chromosomes and cytoskeletal forces essential for homolog pairing. Dev Cell 21, 948–958.

La Salle S, Sun F, Handel MA (2009). Isolation and short-term culture of mouse spermatocytes for analysis of meiosis. Methods Mol Biol 558, 279–297.

Lee HS, Min S, Jung YE, Chae S, Heo J, Lee JH, Kim T, Kang HC, Nakanish M, Cha SS, et al. (2021). Spatiotemporal coordination of the RSF1-PLK1-Aurora B cascade establishes mitotic signaling platforms. Nat Commun 12, 5931.

Li Z, Li J, Kong Y, Yan S, Ahmad N, Liu X (2017). Plk1 phosphorylation of mre11 antagonizes the DNA damage response. Cancer Res 77, 3169–3180.

Lin Q, Inselman A, Han X, Xu H, Zhang W, Handel MA, Skoultchi AI (2004). Reductions in linker histone levels are tolerated in developing spermatocytes but cause changes in specific gene expression. J Biol Chem 279, 23525–23535.

Lipkin SM, Moens PB, Wang V, Lenzi M, Shanmugarajah D, Gilgeous A, Thomas J, Cheng J, Touchman JW, Green ED, et al. (2002). Meiotic arrest and aneuploidy in MLH3-deficient mice. Nat Genet 31, 385–390.

Little TM, Jordan PW (2020). PLK1 is required for chromosome compaction and microtubule organization in mouse oocytes. Mol Biol Cell 31, 1206–1217.

Lu L-Y, Wood JL, Minter-Dykhouse K, Ye L, Saunders TL, Yu X, Chen J (2008). Polo-like kinase 1 is essential for early embryonic development and tumor suppression. Mol Cell Biol 28, 6870–6876.

Luo M, Yang F, Leu NA, Landaiche J, Handel MA, Benavente R, La Salle S, Wang PJ (2013). MEIOB exhibits single-stranded DNA-binding and exonuclease activities and is essential for meiotic recombination. Nat Commun 4, 2788.

Lyndaker AM, Lim PX, Mleczko JM, Diggins CE, Holloway JK, Holmes RJ, Kan R, Schlafer DH, Freire R, Cohen PE, et al. (2013). Conditional inactivation of the DNA damage response gene Hus1 in mouse testis reveals separable roles for components of the RAD9-RAD1-HUS1 complex in meiotic chromosome maintenance. PLoS Genet 9, e1003320.

Machovina TS, Mainpal R, Daryabeigi A, McGovern O, Paouneskou D, Labella S, Zetka M, Jantsch V, Yanowitz JL (2016). A surveillance system ensures crossover formation in C. elegans. Curr Biol 26, 2873–2884.

Matos J, Blanco MG, Maslen S, Skehel JM, West SC (2011). Regulatory control of the resolution of DNA recombination intermediates during meiosis and mitosis. Cell 147, 158–172.

McMahill MS, Sham CW, Bishop DK (2007). Synthesis-dependent strand annealing in meiosis. PLoS Biol 5, e299.

Nadarajan S, Lambert TJ, Altendorfer E, Gao J, Blower MD, Waters JC, Colaiácovo MP (2017). Polo-like kinase-dependent phosphorylation of the synaptonemal complex protein SYP-4 regulates double-strand break formation through a negative feedback loop. Elife 6, e23437.

Parra MT, Gómez R, Viera A, Llano E, Pendás AM, Rufas JS, Suja JA (2009). Sequential assembly of centromeric proteins in male mouse meiosis. PLoS Genet 5, e1000417.

Parra MT, Viera A, Gómez R, Page J, Carmena M, Earnshaw WC, Rufas JS, Suja JA (2003). Dynamic relocalization of the chromosomal passenger complex proteins inner centromere protein (INCENP) and aurora-B kinase during male mouse meiosis. J Cell Sci 116, 961–974.

Qiao H, Chen JK, Reynolds A, Höög C, Paddy M, Hunter N (2012). Interplay between synaptonemal complex, homologous recombination, centromeres during mammalian meiosis. PLoS Genet 8, e1002790.

Refolio E, Cavero S, Marcon E, Freire R, San-Segundo PA (2011). The Ddc2/ATRIP checkpoint protein monitors meiotic recombination intermediates. J Cell Sci 124, 2488–2500.

Reynolds A, Qiao H, Yang Y, Chen JK, Jackson N, Biswas K, Holloway JK, Baudat F, de Massy B, Wang J, et al. (2013). RNF212 is a dosage-sensitive regulator of crossing-over during mammalian meiosis. Nat Genet 45, 269–278.

Robert T, Vrielynck N, Mézard C, de Massy B, Grelon M (2016). A new light on the meiotic DSB catalytic complex. Semin Cell Dev Biol 54, 165–176.

Royo H, Prosser H, Ruzankina Y, Mahadevaiah SK, Cloutier JM, Baumann M, Fukuda T, Höög C, Tóth A, de Rooij DG, et al. (2013). ATR acts stage specifically to regulate multiple aspects of mammalian meiotic silencing. Genes Dev 27, 1484–1494.

Salimian K, Ballister E, Smoak E, Wood S, Panchenko T, Lampson M, Black B (2011). Feedback control in sensing chromosome biorientation by the Aurora B kinase. Curr Biol 21, 1158–1165.

Sanchez A, Adam C, Rauh F, Duroc Y, Ranjha L, Lombard B, Mu X, Wintrebert M, Loew D, Guarné A, et al. (2020). Exo1 recruits Cdc5 polo kinase to MutLγ to ensure efficient meiotic crossover formation. Proc Natl Acad Sci USA 117, 30577–30588.

Sansam CL, Pezza RJ (2015). Connecting by breaking and repairing: mechanisms of DNA strand exchange in meiotic recombination. FEBS J 282, 2444–2457.

Santucci-Darmanin S, Walpita D, Lespinasse F, Desnuelle C, Ashley T, Paquis-Flucklinger V (2000). MSH4 acts in conjunction with MLH1 during mammalian meiosis. FASEB J 14, 1539–1547.

Sheridan S, Bishop DK (2006). Red-Hed regulation: recombinase Rad51, though capable of playing the leading role, may be relegated to supporting Dmc1 in budding yeast meiosis. Genes Dev 20, 1685–1691.

Shi B, Xue J, Yin H, Guo R, Luo M, Ye L, Shi Q, Huang X, Liu M, Sha J, *et al.* (2019). Dual functions for the ssDNA-binding protein RPA in meiotic recombination. PLoS Genet 15, e1007952.

Shinohara M, Oh SD, Hunter N, Shinohara A (2008). Crossover assurance and crossover interference are distinctly regulated by the ZMM proteins during yeast meiosis. Nat Genet 40, 299–309.

Sourirajan A, Lichten M (2008). Polo-like kinase Cdc5 drives exit from pachytene during budding yeast meiosis. Genes Dev 22, 2627–2632.

Stanzione M, Baumann M, Papanikos F, Dereli I, Lange J, Ramlal A, Tränkner D, Shibuya H, de Massy B, Watanabe Y, *et al.* (2016). Meiotic DNA break formation requires the unsynapsed chromosome axis-binding protein IHO1 (CCDC36) in mice. Nat Cell Biol 18, 1208–1220.

Sun F, Handel MA (2008). Regulation of the meiotic prophase I to metaphase I transition in mouse spermatocytes. Chromosoma 117, 471–485.

Svendsen JM, Smogorzewska A, Sowa ME, O'Connell BC, Gygi SP, Elledge SJ, Harper JW (2009). Mammalian BTBD12/SLX4 assembles a Holliday junction resolvase and is required for DNA repair. Cell 138, 63–77.

Szostak JW, Orr-Weaver TL, Rothstein RJ, Stahl FW (1983). The double-strand-break repair model for recombination. Cell 33, 25–35.

Tang C-JC, Lin C-Y, Tang TK (2006). Dynamic localization and functional implications of Aurora-C kinase during male mouse meiosis. Dev Biol 290, 398–410.

Ward JD, Barber LJ, Petalcorin MI, Yanowitz J, Boulton SJ (2007). Replication blocking lesions present a unique substrate for homologous recombination. EMBO J 26, 3384–3396.

Wellard SR, Schindler K, Jordan PW (2020). Aurora B and C kinases regulate chromosome desynapsis and segregation during mouse and human spermatogenesis. J Cell Sci 133.

Wellard SR, Zhang Y, Shults C, Zhao X, McKay M, Murray SA, Jordan PW (2021). Overlapping roles for PLK1 and Aurora A during meiotic centrosome biogenesis in mouse spermatocytes. EMBO Rep 22, e51023.

Wild P, Susperregui A, Piazza I, Dörig C, Oke A, Arter M, Yamaguchi M, Hilditch AT, Vuina K, Chan KC, *et al.* (2019). Network Rewiring of Homologous Recombination Enzymes during Mitotic Proliferation and Meiosis. Mol Cell 75, 859–874.e4.

Wiltshire T, Park C, Caldwell KA, Handel MA (1995). Induced premature G2/M-phase transition in pachytene spermatocytes includes events unique to meiosis. Dev Biol 169, 557–567.

Wyatt HDM, Sarbajna S, Matos J, West SC (2013). Coordinated actions of SLX1-SLX4 and MUS81-EME1 for Holliday junction resolution in human cells. Mol Cell 52, 234–247.

Yata K, Lloyd J, Maslen S, Bleuyard J-Y, Skehel M, Smerdon SJ, Esashi F (2012). Plk1 and CK2 act in concert to regulate Rad51 during DNA double strand break repair. Mol Cell 45, 371–383.

Zickler D, Kleckner N (1999). Meiotic chrDomosomes: integrating structure and function. Annu Rev Genet 33, 603–754.